Targeted disruption of tyrosinase causes melanin reduction in Carassius auratus cuvieri and its hybrid progeny

Qingfeng Liu, Yanhua Qi, Qiuli Liang, Jia Song, Junmei Liu, Wuhui Li, Yuqin Shu, Min Tao, Chun Zhang, Qinbo Qin, Jing Wang and Shaojun Liu

Citation: SCIENCE CHINA Life Sciences; doi: 10.1007/s11427-018-9404-7

View online: http://engine.scichina.com/doi/10.1007/s11427-018-9404-7

Published by the Science China Press

SCIENCE CHINA
Life Sciences

•RESEARCH PAPER•

https://doi.org/10.1007/s11427-018-9404-7

Targeted disruption of tyrosinase causes melanin reduction in *Carassius auratus cuvieri* and its hybrid progeny

Qingfeng Liu[1,2†], Yanhua Qi[1,2†], Qiuli Liang[1,2†], Jia Song[1,2], Junmei Liu[1,2], Wuhui Li[1,2], Yuqin Shu[1,2], Min Tao[1,2], Chun Zhang[1,2], Qinbo Qin[1,2], Jing Wang[1,2] & Shaojun Liu[1,2*]

[1]*State Key Laboratory of Developmental Biology of Freshwater Fish, Hunan Normal University, Changsha 410081, China;*
[2]*College of Life Sciences, Hunan Normal University, Changsha 410081, China*

Received July 22, 2018; accepted October 16, 2018; published online December 27, 2018

The white crucian carp (*Carassius auratus cuvieri*, WCC) not only is one of the most economically important fish in Asia, characterized by strong reproductive ability and rapid growth rates, but also represents a good germplasm to produce hybrid progenies with heterosis. Gene knockout technique provides a safe and acceptant way for fish breeding. Achieving gene knockout in WCC and its hybrid progeny will be of great importance for both genetic studies and hybridization breeding. Tyrosinase (TYR) is a key enzyme in melanin synthesis. Depletion of *tyr* in zebrafish and mice results in mosaic pigmentation or total albinism. Here, we successfully used CRISPR-Cas9 to target *tyr* in WCC and its hybrid progeny (WR) derived from the cross of WCC (♀) and red crucian carp (*Carassius auratus* red var., RCC, ♂). The level of TYR protein was significantly reduced in mutant WCC. Both the mutant WCC and the mutant WR showed different degrees of melanin reduction compared with the wild-type sibling control fish, resulting from different mutation efficiency ranging from 60% to 90%. In addition, the transcriptional expression profiles of a series of pivotal pigment synthesis genes, i.e. *tyrp1*, *mitfa*, *mitfb*, *dct* and *sox10*, were down-regulated in *tyr*-CRISPR WCC, which ultimately caused a reduction in melanin synthesis. These results demonstrated that *tyr* plays a key role in melanin synthesis in WCC and WR, and CRISPR-Cas9 is an effective tool for modifying the genome of economical fish. Furthermore, the *tyr*-CRISPR models could be valuable in understanding fundamental mechanisms of pigment formation in non-model fish.

white crucian carp, hybridization, CRISPR-Cas9, tyrosinase, pigmentation

Citation: Liu, Q., Qi, Y., Liang, Q., Song, J., Liu, J., Li, W., Shu, Y., Tao, M., Zhang, C., Qin, Q., et al. (2018). Targeted disruption of tyrosinase causes melanin reduction in *Carassius auratus cuvieri* and its hybrid progeny. Sci China Life Sci 61, https://doi.org/10.1007/s11427-018-9404-7

INTRODUCTION

The white crucian carp (*Carassius auratus cuvieri*, WCC) is an important economical fish belonging to Cyprinidae (genus *Carassius*) and possesses 100 chromosomes (2*n*=100). WCC is characterized by a high body, small head, short tail, strong reproductive ability, rapid growth rates and spawn only once a year (Wang et al., 2015). In addition, WCC represents a good germplasm with which to produce hybrid progenies with heterosis (Luo et al., 2011). Hybridization, defined as a cross between two genetically differentiated strains or species, facilitates the transfer of genomes between strains or species and gives rise to phenotypic and genotypic changes in the resulting progeny (Chen, 2007; Zhang et al., 2014). This breeding technique is widely used for the genetic breeding of fish to produce progeny that exhibit hybrid vigor or positive heterosis (Bartley et al., 2000). These hybrid progenies usually serve as a rational model for studying genetics, evolution, development, physiology, nutrition and transgenics (Guo et al.,

†Contributed equally to this work.
*Corresponding author (email: lsj@hunnu.edu.cn)

2006; Liu et al., 2007; Xu et al., 2015; Yu et al., 2011). In our previous study (Wang et al., 2015; Liu et al., 2018), we created a hybrid population (WR) by crossing of WCC (♀) and red crucian carp (*Carassius auratus* red var., RCC, ♂). The morphology and genetic composition of WR exhibited obvious hybrid traits. In particular, the body color of WR was gray in adulthood, which was different from its female parent-WCC (silver) and its male parent-RCC (red) (Wang et al., 2015).

Gene knockout technique provides a safe and acceptant way to investigate fish genetics and breeding. Most recently, a revolutionary site-specific genomic-editing technology based on the type II prokaryotic CRISPR (clustered regularly interspaced short palindromic repeats) adaptive immune system has been developed (Hwang et al., 2013; Li et al., 2013). The CRISPR-Cas9 system consists of the Cas9 nuclease and guide RNA (gRNA); the gRNA is responsible for DNA-recognizing/binding while the Cas9 endonuclease acts to cleave DNAs (Chang et al., 2013). In zygotes, the gRNA and the Cas9 protein can cause site-specifice DNA double-strand breaks (DSBs) that induce non-homologous end joining (NHEJ) or homology-directed repair (HDR), resulting in indel mutations in target genes (Hwang et al., 2013). After the initial development of a programmable CRISPR-Cas9 system, it has been rapidly applied to achieve efficient genome editing in human cell, zebrafish, mouse, rat, bacteria and plants (Bikard et al., 2013; Feng et al., 2013; Hwang et al., 2013; Ma et al., 2013; Shen et al., 2013), and in a range of fields, including cancer treatment, human genetic disease, basic research, and animal/agricultural husbandry (Zhen et al., 2014; Men et al., 2017; Zhong et al., 2016). Moreover, the CRISPR-Cas9 system allows for mutagenizing multiple genes in the stem cells or zygotes, and generating bialleic mutants with clear phenotypes in the F_0 generation for studying gene functions without crossing animals for several generations (Cong et al., 2013; Jao et al., 2013; Wang et al., 2013; Yang et al., 2013). However, as yet, there has been no successful application of this system in WCC and its hybrids.

In order to achieve the application of gene editing technology in WCC and WR, and evaluate the melanin formation mechanism of WCC and WR. We employed the CRISPR-Cas9 system to modify the tyrosinase (TYR) in WCC and WR. Tyr is a key enzyme in the melanin biosynthetic pathway and mutations in the *tyr* gene can result in oculocutaneous albinism (OCA) (Oetting and King 1999). Previous research showed that *tyr* knockout mice displayed both a mosaic color and total albinism within 9 d of birth (Zhang et al., 2016). Bi allelic disruption of *tyr* zebrafish embryos resulted in mosaic pigmentation patterns, some of which were almost unpigmented (Jao et al., 2013).

Our present results showed that the skin of *tyr*-CRISPR WCC and WR displayed differing degrees of melanin reduction in both embryos and the juvenile stage. The transcriptional levels of a series of pivotal genes responsible for the synthesis of pigment in skin tissue were analyzed by quantitative polymerase chain reaction (PCR) which demonstrated clear down-regulation in *tyr*-CRISPR WCC. Taken together, these results demonstrate that the CRISPR-Cas9 system is an effective genome-editing tool for WCC and its hybrids for studying genetic and breeding; and the *tyr* gene plays an important and same role in the synthesis of melanin synthesis in WCC and WR.

RESULTS

Body color and electron microscopic analysis of tail fin among WCC, RCC, and WR

The result of electron microscopic of WCC tail showed that WCC with much melanin (Figure 1D). The result of electron microscopic of RCC tail showed that RCC with no melanin (Figure 1E). The result of electron microscopic of WR tail showed that WR with less melanin (Figure 1F). In short, the melanin content in WR body is lower than that in WCC but higher than that in RCC (Figure 1D–F); therefore, the gray body color was a hybrid trait (Figure 1C), which was different from its female parent-WCC (silver) (Figure 1A) and its male parent-RCC (red) (Figure 1B).

Design of the CRISPR-Cas9 target site

We obtained *tyr* cDNA sequences of WCC and WR by PCR; analysis using BioEdit showed that the homology between

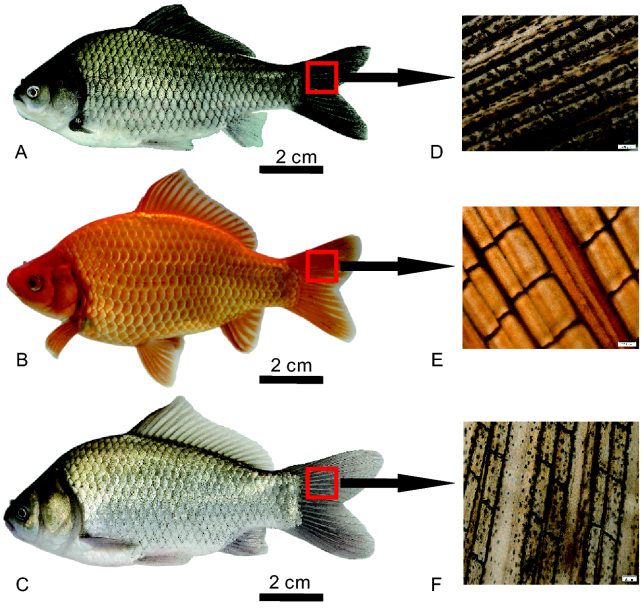

Figure 1 Body color and electron microscopic analysis of tail fin among WCC, RCC, and WR. A, The image of WCC with silver color. B, The image of RCC with red color. C, The image of WR with gray color. D, WCC with much melanin. E, RCC with no melanin. F, WR with less melanin.

these two sequences was 99.57%. The *tyr* sequences of WCC and WR were then BLAST searched against the *tyr* sequence of zebrafish in order to predict exon-intron structure. A target site was obtained from the first exon of the *tyr* gene using the ZiFiT Targeter website (Figure 2A), which was suitable for both WCC and WR. In addition, the selected target site was BLAST searched against the goldfish genome with a reciprocal top BLAST hit for the target regions to minimize off-target effects. The target site included a 20-bp sequence and the protospacer-adjacent motif (PAM) sequence.

Mutagenesis detection and efficiency of CRISPR-Cas9 in WCC and WR

Cas9 mRNA (300 ng μL^{-1}) plus the gRNA (30 ng μL^{-1}) of *tyr* gene was co-microinjected into one-cell WCC and WR embryos using TransferMan NI2 (Eppendorf, Hamburg, Germany), respectively. Each embryo was injected with 2 nL of the solution. To generate *tyr*-CRISPR targeted WCC and WR, 200 additional embryos were microinjected for each group. DNA fragments harboring the target site were amplified by PCR from the tail fin of 2-month-old mutant WCC and WR. When compared with the WT, the PCR products of mutant WCC and WR showed multiple peaks near the PAM sequence (Figure 2B). Sequences of single clones from WCC and WR revealed the deletion or insertion of some bases. WCC specimens had four mutant types while the WR possessed three mutant types (Figure 2C). To examine the efficiency of CRISPR-Cas9-induced mutations, 320 single clones from eight mutant WCC and eight mutant WR were sequenced. Data showed that the mutation efficiency was 79.38% (127 out of the 160 clones) for WCC and 78.13% (126 out of the 160 clones) for WR (Table S1 in Supporting Information). These results demonstrated the feasibility of

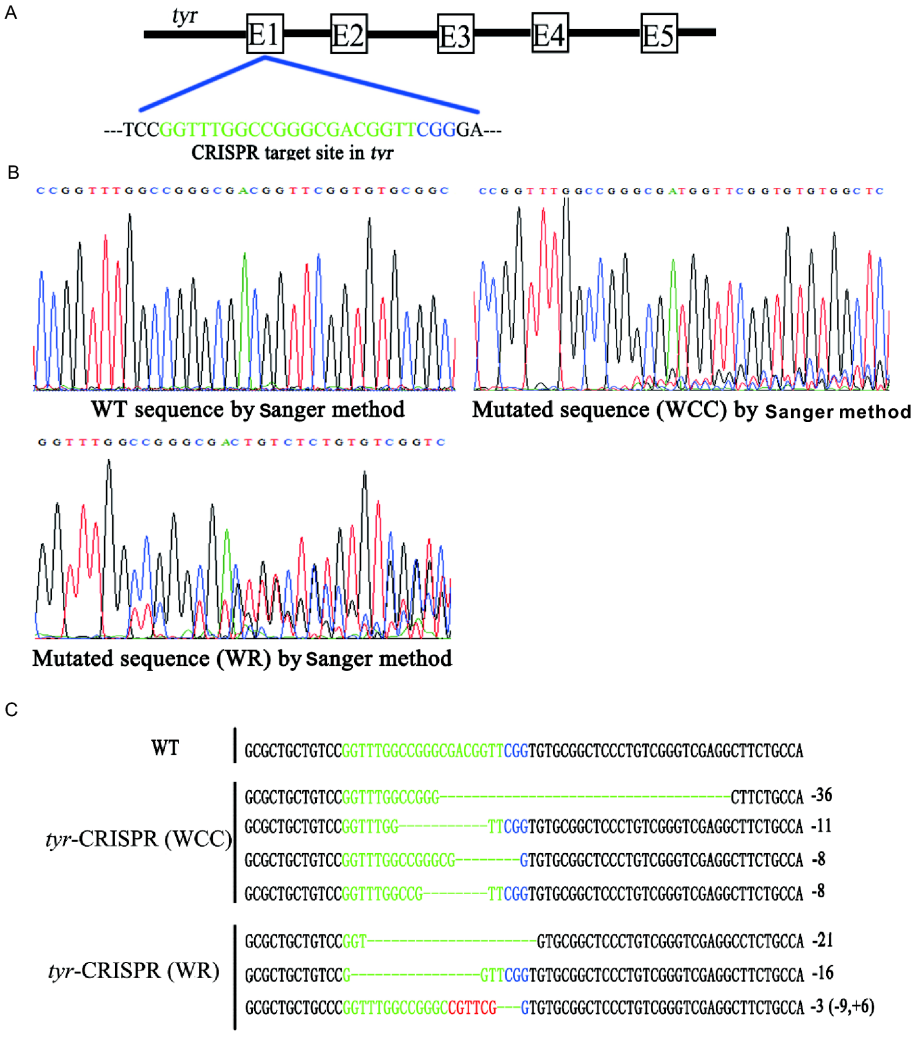

Figure 2 Disruption of WCC and WR *tyr* gene by CRISPR-Cas9. CRISPR-Cas9-induced mutagenesis of the *tyr* gene in WCC and WR. A, Schematic of the CRISPR target site in the WCC and WR *tyr* gene. Target sites are marked with green. The PAM sequence is labeled in blue. E: exon. B, PCR products of mutant WCC and WR showing multiple peaks near to the PAM sequence compared with their WTs, as revealed by the sequencing and analysis of PCR products. C, Four and three types of mutation in WCC and WR respectively, revealed by single clone sequencing analysis. Deleted bases are shown as green dashes. Inserted bases are labeled in red.

using CRISPR-Cas9 to edit target genes in hybrid fish.

Melanin diminished in *tyr* mutant WCC and WR

We selected 30 fishes in each of the injected WCC and WR, which included 20 mutant WCC (66.67%) and 20 mutant WR (66.67%). To ensure the accuracy of our experiment, the mutant WCC, mutant WR, and their respective wild type siblings, were raised separately in the ponds under the same conditions. The body color of the mutant WCC, mutant WR, and their respective control fish were observed at 4 days post fertilization (dpf) and 120 dpf. The mutant WCC and WR showed obvious reductions in melanin compared with their respective WTs, so that some mutant WCC and WR showed pink (Figures 3 and 4). We selected *tyr*-CRISPR WCC with 90% mutation efficiency as high-rate subgroup (Figure 5A), *tyr*-CRISPR WCC with 80% mutation efficiency as middle-rate subgroup (Figure 5B), *tyr*-CRISPR WCC with 60% mutation efficiency as low-rate subgroup (Figure 5C). The melanin content of the body was significantly reduced in the high-rate subgroup compared with that in the middle-rate subgroup, and in the middle-rate subgroup compared with

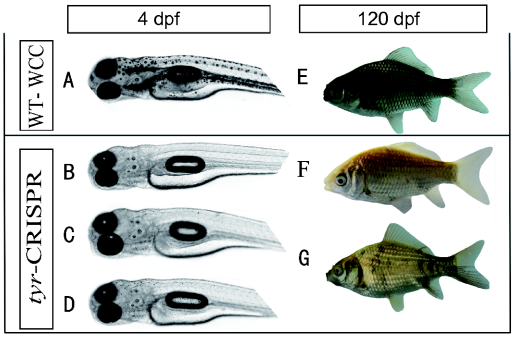

Figure 3 Disruption of tyrosinase (*tyr*) by CRISPR-Cas9 generates reduced melanin phenotypes in WCC. A–D, WT-WCC with obvious melanin (A) and *tyr*-CRISPR WCC with little melanin at 4 dpf (B–D). E–G, WT-WCC in black (E), *tyr*-CRISPR WCC with absolute albinism and showed pink (F), *tyr*-CRISPR WCC with mosaic melanin at 120 dpf (G).

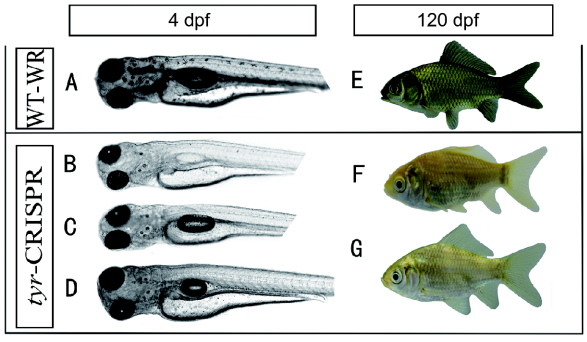

Figure 4 Disruption of tyrosinase (*tyr*) by CRISPR-Cas9 generates reduced melanin phenotypes in WR. A–D, WT-WR with obvious melanin (A) and *tyr*-CRISPR WR with little melanin at 4 dpf (B–D). E–G, WT-WR in gray (E), *tyr*-CRISPR WR with absolute albinism and showed pink (F), *tyr*-CRISPR WR with mosaic melanin at 120 dpf (G).

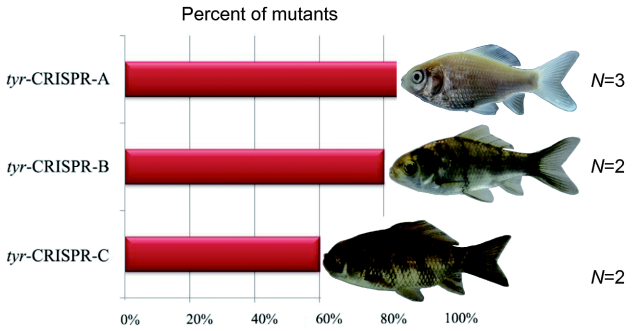

Figure 5 Comparisons of the melanin content in different genotypes of *tyr*-CRISPR WCC. *tyr*-CRISPR-A represents high-rate subgroup with 90% mutation efficiency, *tyr*-CRISPR-B represents middle-rate subgroup with 80% mutation efficiency, *tyr*-CRISPR-C represents low-rate subgroup with 60% mutation efficiency. *N* represents the number of *tyr*-CRISPR WCC.

that in the low-rate subgroup, showing that its level in the body exhibits a phenotype-genotype correlation: the higher the mutation rate (high-rate subgroup), the lower the concentration of melanin in the body. The level of TYR was studied by Western blotting. Protein was extracted from the skin of 120 dpf WT control WCC, and mutation WCC with high mutation rate. Results showed that no TYR protein was detected in the *tyr*-CRISPR WR compared with that in the WT controls, implying that CRISPR-Cas9-induced mutations affect the normal expression of TYR protein (Figure 6). Moreover, we used an electron microscope to observe color changes in the skin and tail in more detail and to allow specific comparison between mutant WCC and WT control WCC. This showed a clear reduction of melanin in the mutant WCC compared with that in the WT control WCC (Figure 7).

Mutation of *tyr* caused the down-regulation of pivotal pigment synthesis genes in mutant WCC

To determine if *tyr* depletion affected the expression of other pigment genes (Zhu et al., 2016) in mutant WCC, the transcriptional levels of *tyr*, *tyrp1*, *dct*, *mitfa*, *mitfb* and *sox10* were analyzed by quantitative PCR. RNA was extracted from the skin of 120 dpf WT control WCC and mutant WCC with a high mutation rate. The expression levels of *tyr*, *tyrp1*, *dct*, *mitfa*, *mitfb* and *sox10* in mutant WCC were all significantly down-regulated compared with WT control WCC (Figure 8).

DISCUSSION

Until now, targeted gene editing has been reported in zebrafish (Hwang et al., 2013), medaka (Chen et al., 2016), rice field eel (*Monopterus albus*) (Feng et al., 2017), starlet (*Acipenser ruthenus*) (Chen et al., 2018), Nile tilapia (Li et al., 2014), rainbow trout (Yano et al., 2014), common carp (Chakrapani et al., 2016), channel catfish (Liu et al., 2016),

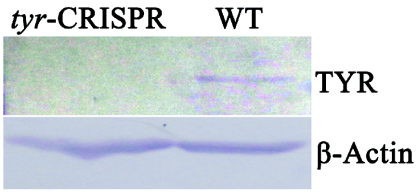

Figure 6 Western blotting analysis of TYR in WT and *tyr*-CRISPR WCC. No TYR protein was detected in the *tyr*-CRISPR WCC with high mutation rate (left) when compared with the WT control (right).

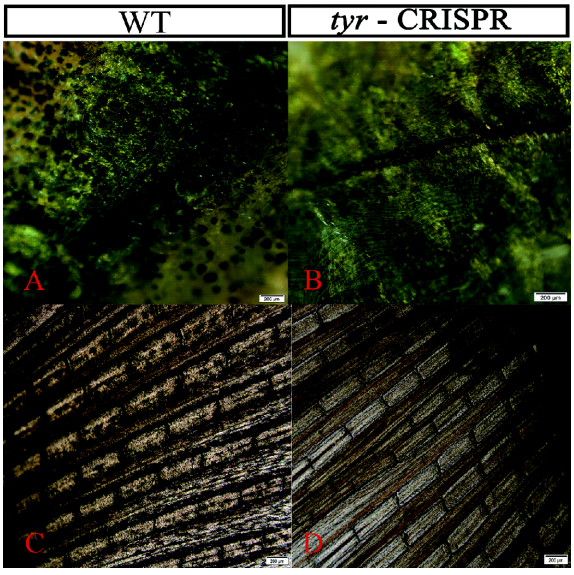

Figure 7 Electron microscopy observation of the skin and tail fin from WT and *tyr*-CRISPR WCC. A, The skin of WT WCC with much melanin. B, The skin of *tyr*-CRISPR WCC without melanin. C, The tail fin of WT WCC full of melanin. D, The tail fin of *tyr*-CRISPR WCC without melanin.

Chinese tongue sole (*Cynoglossus semilaevis*) (Cui et al., 2017), and so on. However, the use of genome editing tools has been rarely used in WCC and hybrid fish. In this study, we successfully generated a *tyr* gene knockout WCC and WR using the genomic-editing technology CRISPR-Cas9. And, we observed a change of phenotype in the *tyr*-CRISPR WCC and WR compared with that in their WT sibling controls. The successful application of CRISPR-Cas9 in the WCC and WR opens an exciting range of avenues for facilitating the study of genetics and breeding in freshwater fish. Firstly, the technique is applicable for genes that function in later stages of development, or in adulthood, such as ageing genes, mature osteoblast genes and circadian clock genes (Zhong et al., 2016). Furthermore, in order to preserve the advantages of hybrid fish, heterosis-related genes can be determined by knockout, such as the growth hormone receptor (*ghr*), insulin like growth factor 2 (*igf2*) and myostatin (*mstn*) genes, which are associated with growth and were previously shown to be differentially expressed in diploid and allotetraploid hybrids of RCC and common carp (Ren et al., 2016). Finally, we can also apply the combination of gene knockout technique and hybridization technique to fish genetic breeding. For example, we can use CRISPR-Cas9 system to knock out muscle suppressor gene *mstn* in WR, so that WR possess more advantages.

Color patterns in fish skin play an important role in numerous biological processes, such as camouflage, mate choice, and the perception of threatening behavior (Kelsh, 2004; Protas and Patel, 2008). However, the method responsible for skin color formation in fish has been a source of debate among biologists for some time and may be associated with a series of genetic, cellular, environmental and physiological factors (Aspengren et al., 2009). In the present study, the body color of WR is a hybrid trait (Figure 1D–F), which provides a good system for us to study fish skin color. Thus far, a series of genes have been reported to be involved in the determination of skin color, such as pro-opiomelanocortin (*pomc*), melanocytestimulating hormone (*msh*), microphthalmia-associated transcription factor (*mitf*), kit oncogene (*kit*), and *tyr* (Hubbard et al., 2010; Kelsh, 2004). In particular, the *tyr* gene has been shown to play a key role in the biosynthesis of melanin (Oetting and King, 1999).

We cloned WCC and WR *tyr* cDNA sequences and edited the *tyr* gene in WCC and WR to investigate the *tyr* gene function both in WCC and WR. According to our results (Figures 3 and 4), the *ty*r-CRISPR WCC and *ty*r-CRISPR WR both showed different degrees of melanin reduction compared with their WT sibling controls. The finding was consistent with previous studies in zebrafish and mice (Jao et al., 2013; Zhang et al., 2016). It suggested that the *tyr* is a fairly conservative gene in different species and even in a new hybrid species; and the hybrid progeny (WR) has the same regulation mode of melanin with WCC. In addition, these phenotypes (Figure 5) were similar with previous research describing individuals with OCA1 caused by *tyr* mutation; individuals with OCA1A show a complete lack of pigment through their life, while other individuals with OCA1B possessed mutations that resulted in residual tyrosinase activity, producing a spectrum in the amount of pigment in the skin, hair, and eyes (Oetting and King, 1999). So, on the basis of previous study, we provided further explanation for the albinism: both the mutation rates and mutation sites of *tyr* can influence the activity of tyrosinase, so that the reduction of melanin.

Finally, we measured the expression of key pigment-related genes in *tyr*-CRISPR WCC skin tissue using quantitative PCR. Our results showed that the expression levels of *tyr*, *tyrp1*, *dct*, *mitfa*, *mitfb* and *sox10* were significantly down-regulated (Figure 8), which caused a reduction in melanin synthesis (Braasch et al., 2009; Li et al., 2012). In particular, the expression of *mitfa*, a key regulator for pigment, and the upstream gene for *tyr*, *tyrp1* and *dct* (Nishimura et al., 2002; Altschmied et al., 2002), was down-regulated in mutant WCC. This finding suggested that less

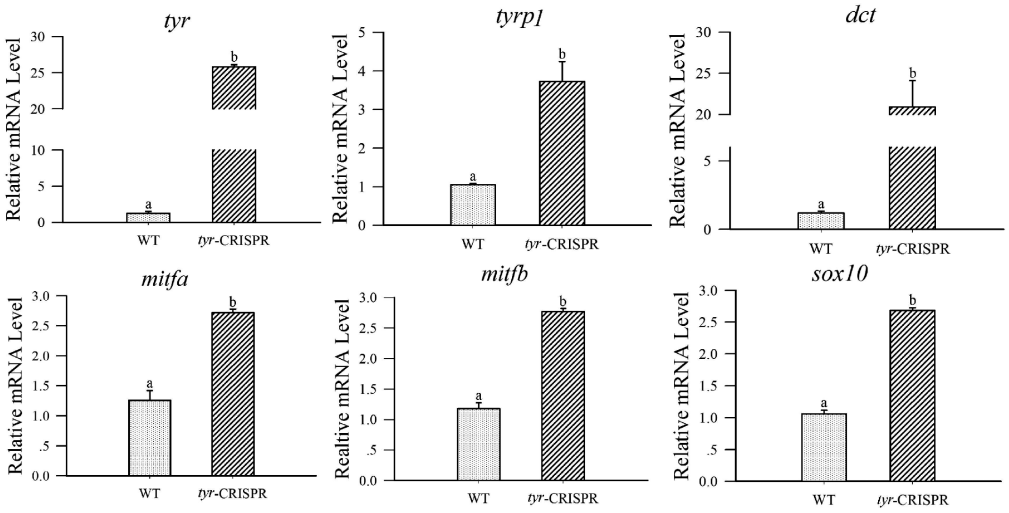

Figure 8 Transcriptional expression levels of six pigment genes in *tyr*-CRISPR WCC and WT. In each panel, different lowercase letters indicate significant differences ($P<0.05$).

melanin was synthesized in the *tyr*-CRISPR WCC may be caused by the co-action of these key pigment genes, and it also provided a view that deletion of the *tyr* gene may influence the expression of *mitf*. In the future, we will further explore the mechanisms of melanin reduction.

In summary, our studies demonstrate that CRISPR-Cas9 is an effective tool for genetics studies in WCC and its hybrid fish, which will promote genetic engineering in aquaculture and is likely to play a significant role in the improvement of fish quality and economic value. Furthermore, the *tyr*-CRISPR models generated herein are of significant value in understanding the fundamental mechanisms of pigment patterns formation in non-model fish. To our knowledge, this is the first paper to report the targeted disruption of endogenous genes in WCC and its hybrids using CRISPR-Cas9.

MATERIALS AND METHODS

Ethics statement

Animal care and experimenters were certified by a professional training course for laboratory animal practitioners held by the Institute of Experimental Animals, Hunan Province, China.

Gene cloning and sequencing

To isolate WCC and WR *tyr* cDNA sequences, we designed primers (Table S2 in Supporting Information) based on the *tyr* gene of RCC (accession number: AB334215.1). PCR was performed using these primers and products were separated on a 1.2% agarose gel, purified using a Gel Extraction Kit (Sangon Biotech Co., Ltd., Shanghai, China), ligated into a pMD18-T vector, and finally transferred into *E. coli* DH5α. Positive clones were screened by colony PCR and sequenced. Finally, sequences were aligned using BioEdit (Hall, 1999).

Design of the CRISPR-Cas9 target site

The gRNA for CRISPR-Cas9 was designed using the ZiFiT Targeter website according to the 5′-GGNNNNNNNN-NNNNNNNNNNNGG-3′ roles (Hwang et al., 2013). The first two G were necessary for the T7 RNA polymerase and the end NGG was the protospacer-adjacent motif (PAM). The minmal number of nucleotides (N) was 19 bp depending on the sequence of the *tyr* gene.

Production of gRNA and Cas9 mRNA

gRNA and Cas9 mRNA were synthesized as described previously (Hwang et al., 2013). In brief, the DNA template for gRNA was generated by PCR with a pair of primers (Table S2 in Supporting Information), and then purified using phenol and chloroform. gRNA was then *in vitro* transcribed using the MAXIscript T7 kit (Ambion, CA, USA) according to the manufacturer's protocol. The Cas9 mRNA was then transcribed using the *Xba* I-digested vector and the mMESSAGE mMACHINE T7 ULTRA kit (Ambion, CA, USA) according to the manufacturer's protocol. Both the gRNA and the Cas9-encoding mRNA were then purified by LiCl precipitation and re-dissolved in RNase-free water.

Microinjection of WCC and WR embryos

WCC and WR embryos were collected from the State Key Laboratory of Developmental Biology of Freshwater Fish, Hunan Normal University, Changsha, China during the reproductive season (from April to June). The protocol for

crosses was described previously (Wang et al., 2015). A mixture of Cas9 mRNA (300 ng μL^{-1}) and gRNA (30 ng μL^{-1}) was injected into embryos 15 min after fertilization. Embryos were allowed to develop in culture dishes at a water temperature of 19–22°C. Juveniles were housed at an appropriate density in a 0.067-ha open pool. The pH range of the water was 7.0–8.5 and the dissolved oxygen range was 5.0–8.0 mg L^{-1}.

Mutagenesis detection assays and efficiency analyses

DNA fragments containing the targeted site was amplified by PCR with DNAs extracted from the tail fin of 2-month-old WCC and WR with melanin reduction. First, the PCR products were purified and directly sequenced to reveal the presence of double peaks or indels. Next, the purified PCR products were ligated into a pMD18-T vector, and transferred into *E. coli* DH5α cells. A single clone was picked up, amplified by PCR and sequenced to verify mutated sequences and determine mutational efficiencies. The mutated sequences were from single WCC and WR individuals. Five WCC and five WR were chosen to calculate their respective mutational efficiency. The primers used for PCR amplification with DNAs are listed in Table S2 in Supporting Information.

Total RNA isolation and gene expression levels quantified with real-time PCR analyses

Total RNAs were extracted from the skin of *tyr*-CRISPR mutated WCC with TriZol (Invitrogen, CA, USA) and used for quantitative PCR (qPCR) analysis. Real-time PCR analysis was then performed using the Prism 7500 Sequence Detection System (Ambion, CA, USA) with a miScript SYBR Green PCR kit (Qiagen, Duesseldorf, Germany). The amplification conditions were as follows: 50°C for 5 min and 95°C for 10 min, followed by 40 cycles at 95°C for 15 s and 60°C for 45 s. Real-time qPCR was performed on biological replicates in triplicate (and triplicate technical qPCR replicates). All results were normalized to the expression level of the housekeeping gene β-actin and were determined as a relative expression level calculated using the $2^{-\Delta\Delta C_t}$ method. Primers for *tyr*, *tyrp1*, *mitfa*, *mitfb*, *dct* and *sox10* are listed inTable S2 in Supporting Information.

Western blotting

Protein samples were collected from the skin of 120 dpf mutated WCC, and wild-type (WT) WCC, using a tissue total protein extraction kit (Sangon Biotech, Wuhan, China). In brief, the same amount of protein was isolated by 8% sodium dodecyl sulfate polyacrylamide gel electrophoresis (SDS-PAGE) and transferred onto polyvinylidene fluoride (PVDF) membranes (Millipore). After blocking, the PVDF membranes were separately incubated with an anti-TYR rabbit polyclonal antibody (1:800; BBI life sciences, Wuhan, China) or mouse-anti-actin antibody (1:4000; Sigma, USA). Then, the membrane was washed and separately incubated with goat-anti-mouse or goat-anti-rabbit IgG (1:30000; Sigma, USA). Target proteins were then visualized with a BCIP/NBT Alkaline Phosphatase Color Development Kit (Sigma, USA).

Electron microscopic analysis of skin and tail fin

The skin and tail fin of *tyr*-CRISPR mutated WCC and the tail of WCC, RCC and WR were quickly dissected, soaked in phosphate buffer solution, and directly observed under a Leica inverted CW4000 microscope and a Leica LCS SP2 confocal imaging system (Leica, Germany).

Statistical analysis

Statistical analyses were performed with the unpaired, two-tailed Student's *t*-test or one-way analysis of variance (ANOVA) with the post hoc least significant difference (LSD) method. All statistical analyses were performed using SPSS 16.0 software and $P<0.05$ was regarded as a statistically significant difference.

Compliance and ethics *The author(s) declare that they have no conflict of interest.*

Acknowledgements *This work was supported by the National Natural Science Foundation of China (31430088, 31730098), the earmarked fund for China Agriculture Research System (CARS-45), the Cooperative Innovation Center of Engineering and New Products for Developmental Biology of Hunan Province (20134486), the Natural Science Foundation of Hunan Province (14JJ2062), and the Research Foundation of Education Bureau of Hunan Province, China (16B160).*

Altschmied, J., Delfgaauw, J., Wilde, B., Duschl, J., Bouneau, L., Volff, J. N., Schartl, M. (2002). Subfunctionalization of duplicate mitf genes associated with differential degeneration of alternative exons in fish. Genetics 161, 259–267.

Aspengren, S., Sköld, H.N., and Wallin, M. (2009). Different strategies for color change. Cell Mol Life Sci 66, 187–191.

Bartley, D.M., Rana, K., and Immink, A.J. (2000). The use of inter-specific hybrids in aquaculture and fisheries reviews in fish. Rev Fish Biol Fisheries 10, 325–337.

Bikard, D., Jiang, W., Samai, P., Hochschild, A., Zhang, F., and Marraffini, L.A. (2013). Programmable repression and activation of bacterial gene expression using an engineered CRISPR-Cas system. Nucleic Acids Res 41, 7429–7437.

Braasch, I., Liedtke, D., Volff, J.N., and Schartl, M. (2009). Pigmentary function and evolution of *tyrp1* gene duplicates in fish. Pigm Cell Melanoma Res 22, 839–850.

Chang, N., Sun, C., Gao, L., Zhu, D., Xu, X., Zhu, X., Xiong, J.W., and Xi, J.J. (2013). Genome editing with RNA-guided Cas9 nuclease in Zebrafish embryos. Cell Res 23, 465–472.

Chakrapani, V., Patra, S.K., Panda, R.P., Rasal, K.D., Jayasankar, P., and Barman, H.K. (2016). Establishing targeted carp TLR22 gene disruption via homologous recombination using CRISPR/Cas9. Dev Comp Immunol 61, 242–247.

Chen, J., Cui, X., Jia, S., Luo, D., Cao, M., Zhang, Y., Hu, H., Huang, K., Zhu, Z., and Hu, W. (2016). Disruption of dmc1 produces abnormal sperm in medaka (*Oryzias latipes*). Sci Rep 6, 30912.

Chen, J., Wang, W., Tian, Z., Dong, Y., Dong, T., Zhu, H., Zhu, Z., Hu, H., and Hu, W. (2018). Efficient gene transfer and gene editing in sterlet (acipenser ruthenus). Front Genet 9, 117.

Chen, Z.J. (2007). Genetic and epigenetic mechanisms for gene expression and phenotypic variation in plant polyploids. Annu Rev Plant Biol 58, 377–406.

Cong, L., Ran, F.A., Cox, D., Lin, S., Barretto, R., Habib, N., Hsu, P.D., Wu, X., Jiang, W., Marraffini, L.A., et al. (2013). Multiplex genome engineering using CRISPR/Cas systems. Science 339, 819–823.

Cui, Z., Liu, Y., Wang, W., Wang, Q., Zhang, N., Lin, F., Wang, N., Shao, C., Dong, Z., Li, Y., et al. (2017). Genome editing reveals dmrt1 as an essential male sex-determining gene in Chinese tongue sole (Cynoglossus semilaevis). Sci Rep 7, 42213.

Feng, K., Luo, H., Li, Y., Chen, J., Wang, Y., Sun, Y., Zhu, Z., and Hu, W. (2017). High efficient gene targeting in rice field eel *Monopterus* albus by transcription activator-like effector nucleases. Sci Bull 62, 162–164.

Feng, Z., Zhang, B., Ding, W., Liu, X., Yang, D.L., Wei, P., Cao, F., Zhu, S., Zhang, F., Mao, Y., et al. (2013). Efficient genome editing in plants using a CRISPR/Cas system. Cell Res 23, 1229–1232.

Guo, X., Liu, S., and Liu, Y. (2006). Evidence for recombination of mitochondrial DNA in triploid crucian carp. Genetics 172, 1745–1749.

Hall, T, A. (1999). BioEdit: a user-friendly biological sequence alignment editor and analysis program for Windows 95/98/NT. In: Nucleic Acids Symposium Series, 95–98.

Hubbard, J.K., Uy, J.A.C., Hauber, M.E., Hoekstra, H.E., and Safran, R.J. (2010). Vertebrate pigmentation: from underlying genes to adaptive function. Trends Genets 26, 231–239.

Hwang, W.Y., Fu, Y., Reyon, D., Maeder, M.L., Tsai, S.Q., Sander, J.D., Peterson, R.T., Yeh, J.R.J., and Joung, J.K. (2013). Efficient genome editing in zebrafish using a CRISPR-Cas system. Nat Biotechnol 31, 227–229.

Jao, L.E., Wente, S.R., and Chen, W. (2013). Efficient multiplex biallelic zebrafish genome editing using a CRISPR nuclease system. Proc Natl Acad Sci USA 110, 13904–13909.

Kelsh, R.N. (2004). Genetics and evolution of pigment patterns in fish. Pigment Cell Res 17, 326–336.

Li, D., Qiu, Z., Shao, Y., Chen, Y., Guan, Y., Liu, M., Li, Y., Gao, N., Wang, L., Lu, X., et al. (2013). Heritable gene targeting in the mouse and rat using a CRISPR-Cas system. Nat Biotechnol 31, 681–683.

Li, M., Yang, H., Zhao, J., Fang, L., Shi, H., Li, M., Sun, Y., Zhang, X., Jiang, D., Zhou, L., et al. (2014). Efficient and heritable gene targeting in tilapia by CRISPR/Cas9. Genetics 197, 591–599.

Li, S., Wang, C., Yu, W., Zhao, S., and Gong, Y. (2012). Identification of genes related to white and black plumage formation by RNA-Seq from white and black feather bulbs in ducks. PLoS ONE 7, e36592.

Liu, Q., Qi, Y., Liang, Q., Xu, X., Hu, F., Wang, J., Xiao, J., Wang, S., Li, W., Tao, M., et al. (2018). The chimeric genes in the hybrid lineage of *Carassius auratus cuvieri* (♀)×Carassius auratus red var. (♂). Sci China Life Sci 61, 1079–1089.

Liu, S., Qin, Q., Xiao, J., Lu, W., Shen, J., Li, W., Liu, J., Duan, W., Zhang, C., Tao, M., et al. (2007). The formation of the polyploid hybrids from different subfamily fish crossings and its evolutionary significance. Genetics 176, 1023–1034.

Liu, Z., Liu, S., Yao, J., Bao, L., Zhang, J., Li, Y., Jiang, C., Sun, L., Wang, R., Zhang, Y., et al. (2016). The channel catfish genome sequence provides insights into the evolution of scale formation in teleosts. Nat Commun 7, 11757.

Luo, K.K., Xiao, J., Liu, S.J., Wang, J., He, W.G., Hu, J., Qin, Q.B., Zhang, C., Tao, M., and Liu, Y. (2011). Massive production of all-female diploids and triploids in the crucian carp. Int J Biol Sci 7, 487–495.

Ma, M., Ye, A.Y., Zheng, W., and Kong, L. (2013). A guide RNA sequence design platform for the CRISPR/Cas9 system for model organism genomes. Biomed Res Int 5, 1–4.

Men, K., Duan, X., He, Z., Yang, Y., Yao, S., and Wei, Y. (2017). CRISPR/Cas9-mediated correction of human genetic disease. Sci China Life Sci 60, 447–457.

Nishimura, E.K., Jordan, S.A., Oshima, H., Yoshida, H., Osawa, M., Moriyama, M., Jackson, I.J., Barrandon, Y., Miyachi, Y., and Nishikawa, S.I. (2002). Dominant role of the niche in melanocyte stem-cell fate determination. Nature 416, 854–860.

Oetting, W.S., and King, R.A. (1999). Molecular basis of albinism: mutations and polymorphisms of pigmentation genes associated with albinism. Hum Mutat 13, 99–115.

Protas, M.E., and Patel, N.H. (2008). Evolution of coloration patterns. Annu Rev Cell Dev Biol 24, 425–446.

Ren, L., Li, W., Tao, M., Qin, Q., Luo, J., Chai, J., Tang, C., Xiao, J., Tang, X., Lin, G., et al. (2016). Homoeologue expression insights into the basis of growth heterosis at the intersection of ploidy and hybridity in Cyprinidae. Sci Rep 6, 27040.

Shen, B., Zhang, J., Wu, H., Wang, J., Ma, K., Li, Z., Zhang, X., Zhang, P., and Huang, X. (2013). Generation of gene-modified mice via Cas9/RNA-mediated gene targeting. Cell Res 23, 720–723.

Wang, H., Yang, H., Shivalila, C.S., Dawlaty, M.M., Cheng, A.W., Zhang, F., and Jaenisch, R. (2013). One-step generation of mice carrying mutations in multiple genes by CRISPR/Cas-mediated genome engineering. Cell 153, 910–918.

Wang, J., Xiao, J., Zeng, M., Xu, K., Tao, M., Zhang, C., Duan, W., Liu, W. B., Luo, K.K., Liu, Y., et al. (2015). Genomic variation in the hybrids of white crucian carp and red crucian carp: evidence from ribosomal DNA. Sci China Life Sci 58, 590–601.

Xu, K., Duan, W., Xiao, J., Tao, M., Zhang, C., Liu, Y., and Liu, S.J. (2015). Development and application of biological technologies in fish genetic breeding. Sci China Life Sci 58, 187–201.

Yano, A., Nicol, B., Jouanno, E., and Guiguen, Y. (2014). Heritable targeted inactivation of the rainbow trout (Oncorhynchus mykiss) master sex-determining gene using zinc-finger nucleases. Mar Biotechnol 16, 243–250.

Yang, H., Wang, H., Shivalila, C.S., Cheng, A.W., Shi, L., and Jaenisch, R. (2013). One-step generation of mice carrying reporter and conditional alleles by CRISPR/Cas-mediated genome engineering. Cell 154, 1370–1379.

Yu, F., Xiao, J., Liang, X.Y., Liu, S.J., Zhou, G.J., Luo, K.K., Liu, Y., Hu, W., Wang, Y.P., and Zhu, Z.Y. (2011). Rapid growth and sterility of growth hormone gene transgenic triploid carp. Chin Sci Bull 56, 1679–1684.

Zhang, X., Liang, P., Ding, C., Zhang, Z., Zhou, J., Xie, X., Huang, R., Sun, Y., Sun, H., Zhang, J., et al. (2016). Efficient production of gene-modified mice using staphylococcus aureus Cas9. Sci Rep 6, 32565.

Zhang, Z.H., Chen, J., Li, L., Tao, M., Zhang, C., Qin, Q.B., Xiao, J., Liu, Y., and Liu, S.J. (2014). Research advances in animal distant hybridization. Sci China Life Sci 57, 889–902.

Zhen, S., Hua, L., Takahashi, Y., Narita, S., Liu, Y.H., and Li, Y. (2014). *In vitro* and *in vivo* growth suppression of human papillomavirus 16-positive cervical cancer cells by CRISPR/Cas9. Biochem Biophys Res Commun 450, 1422–1426.

Zhong, Z., Niu, P., Wang, M., Huang, G., Xu, S., Sun, Y., Xu, X., Hou, Y., Sun, X., Yan, Y., et al. (2016). Targeted disruption of sp7 and myostatin with CRISPR-Cas9 results in severe bone defects and more muscular cells in common carp. Sci Rep 6, 22953.

Zhu, W., Wang, L., Dong, Z., Chen, X., Song, F., Liu, N., Yang, H., and Fu, J. (2016). Comparative transcriptome analysis identifies candidate genes related to skin color differentiation in red tilapia. Sci Rep 6, 31347.

SUPPORTING INFORMATION

Table S1 Primer sequences used in the PCR

Table S2 CRISPR-Cas9-induced mutagenesis efficiencies evaluated in WCC and WR

The supporting information is available online at http://life.scichina.com and http://link.springer.com. The supporting materials are published as submitted, without typesetting or editing. The responsibility for scientific accuracy and content remains entirely with the authors.